J. Micropalaeontology, 45, 259–273, 2026
https://doi.org/10.5194/jm-45-259-2026

Journal of Micropalaeontology
Open Access

New material of *Schizopholis* (family Botsfordiidae) from the Tsinghsutung Formation (Cambrian Series 2, Stage 4) in Songtao County, Guizhou Province, South China

Buqing Wei[1,2], Xinglian Yang[1,2], Dezhi Wang[1,2], Weiyi Wu[3], and Yongqin Mao[4]

[1]College of Resources and Environmental Engineering, Guizhou University & Key Laboratory of Karst Georesources and Environment, Ministry of Education (Guizhou University), Guiyang 550025, China
[2]Guizhou Provincial Key Laboratory for Palaeontology and Palaeoenvironment, Guiyang 550025, China
[3]College of Resources and Environmental Engineering, Guizhou Institute of Technology, Guiyang 550003, China
[4]Institute of Mountain Resources, Guizhou Academy of Sciences, Guiyang 550001, China

Correspondence: Xinglian Yang (yangxinglian2002@163.com)

Received: 11 June 2025 – Revised: 8 February 2026 – Accepted: 9 February 2026 – Published: 13 April 2026

Abstract. Organophosphatic brachiopods, widely distributed across several Cambrian tectonic plates, are crucial in understanding the evolution of early brachiopods. Here, we report newly discovered material of *Schizopholis yorkensis* from the Tsinghsutung Formation (Cambrian Series 2, Stage 4) in Songtao County, Guizhou Province, South China. This study presents the first systematic description of *S. yorkensis* from South China and extends its palaeobiogeographical distribution significantly. These specimens obtained through acid etching exhibit well-preserved morphological characteristics, including two tubercles on the dorsal metamorphic shell and three tubercles on the ventral metamorphic shell. Additionally, the ventral valve has divergent delthyrium throughout its ontogeny. Palaeogeographical analysis indicates that *Schizopholis* was predominantly distributed in low-latitude regions and reached its highest diversity level during the Cambrian Age 4, suggesting a phase of rapid spatial expansion during this interval. *Schizopholis yorkensis* was previously known from only North China and Australia during the Cambrian Age 3, but its subsequent distribution implies an expansion to South China and Antarctica during the Cambrian Age 4. In contrast, *S. napuru* is largely restricted to the Cambrian Age 4, providing vital auxiliary information for the palaeobiogeographical and biostratigraphical correlations.

1 Introduction

Brachiopods were one of the most important biotic components of the marine benthic community throughout geological history and played a crucial role in the shaping of the marine ecosystem (Bassett et al., 1999; Carlson, 2016; Harper et al., 2017; Zhang et al., 2018a). The family Botsfordiidae has been proposed as the possible ancestral clade of Acrothelidae (Williams et al., 2000). Among these, *Schizopholis* was previously assigned to Acrothelidae by Williams et al. (2000) and later placed within the family Botsfordiidae by Gravestock et al. (2001) based on the presence of the opening pedicle groove. *Schizopholis* was restudied, and *Karathele* and *Discinolepis* were suggested to be junior synonyms of *Schizopholis* by Popov et al. (2015). The relationships among *Schizopholis* and the other acrotheloids (*Botsfordia*, *Eothele*, and *Acrothele*) have also attracted attention (Holmer et al., 1996; Korovnikov, 1998; Bassett et al., 1999; Gravestock et al., 2001; Popov et al., 2015; Claybourn et al., 2020). Morphologically, *Schizopholis* is similar to *Eothele* and *Acrothele* but differs from the latter two genera in having an open delthyrium instead of an enclosed pedicle foramen (Holmer et al., 1996; Popov et al., 2015; Smith et al., 2015). *Schizopholis* is intermediate between *Botsfordia* and

Eothele in terms of both the morphology and the nature of the pedicle opening, suggesting that it plays a key role in the evolutionary transition from *Botsfordia* to *Schizopholis* to *Eothele* and, eventually, to *Acrothele* (Holmer et al., 1996, 2001; Korovnikov, 1998; Bassett et al., 1999; Popov et al., 2015). Additionally, the main difference between *Schizopholis* and *Botsfordia* is the presence or absence of the median sulcus on the dorsal valve as identified by Claybourn et al. (2020). Phylogenetically, *Schizopholis* is usually found to be a paraphyletic group, connecting the botsfordiids (*Botsfordia* taxon) with the acrothelids (*Eothele*, *Acrothele*, and *Orbithele* taxa) to form a monophyletic group (Claybourn et al., 2020: p. 8, fig. 3).

Schizopholis was first established by Waagen (1885) based on the specimens from the Khussak Formation (lower *Neobolus* beds), Salt Range, Pakistan. To date, *Schizopholis* has been described from carbonate deposits across different palaeocontinents, including Australia, Antarctica, the Himalaya, North China, and Kazakhstan (Kruse, 1990, 1998; Gravestock et al., 2001; Holmer et al., 2001; Popov et al., 2015; Percival and Kruse, 2014; Pan et al., 2019; Claybourn et al., 2020; Popov et al., 2021). In contrast, fossil records of *Schizopholis* from South China have been relatively scarce and are mainly restricted to clastic deposits (Chen et al., 2019; Liu et al., 2020). Moreover, previous studies of Cambrian brachiopod from the Tsinghsutung Formation (Cambrian Series 2, Stage 4) in Guizhou Province have mostly focused on the acrotretoids (Wei et al., 2020, 2023). Only one species of *S. napuru* has been identified from the mudstone layers from the Tsinghsutung Formation in Jianhe County, Guizhou Province (Liu et al., 2020). Here, we present the first systematic description of *S. yorkensis* from the Tsinghsutung Formation in Songtao County, Guizhou Province. The specimens are well preserved and provide important new information, allowing an improved understanding of their morphological and anatomical characteristics. The new material of *S. yorkensis* at the Panxin section in Songtao County also extends the palaeobiogeographical distribution of *Schizopholis* in carbonate sediments of South China.

2 Geological setting

The study area is located in Songtao County, northeast of Tongren City, Guizhou Province (Fig. 1A). During the Cambrian Age 4, it was a part of the shoal of the Yangtze Platform margin (Sang and Wang, 1987; Yin, 1990). The Cambrian strata are widely distributed in the Songtao area, including the Niutitang, Jiumengchong, Bianmachong, Balang, Tsinghsutung, Gaotai, Shilengshui, and Loushanguan formations in ascending order (Fig. 1B; Yin, 1987). The lithology of the Tsinghsutung Formation in the Songtao area comprises mainly thick, grey limestone (upper part) and thin, grey-black argillaceous limestone (lower part; Lin et al., 1966).

The studied Panxin section is located approximately 1 km east of Panxin Town, Songtao County (Fig. 1B), where the Tsinghsutung Formation is incompletely exposed and has a thickness of approximately 84 m (Fig. 1C). The Tsinghsutung Formation comprises grey-black mud-ribbon limestone; grey-black argillaceous limestone; thin, black carbonaceous limestone; and thick, grey-black leopard limestone. The fossil specimens described herein were collected from the Panxin section at 13–51 m above the base of Tsinghsutung Formation (Fig. 1C).

3 Materials and methods

In total, 26 kg of samples (each sample ranges from 0.8 to 1.2 kg) was collected for this study. In the Panxin section, 25 samples were collected from the Tsinghsutung Formation (see black arrows, Fig. 1C). All fossil specimens were extracted from the limestones in the Tsinghsutung Formation outcrop at the Panxin section (Fig. 1C) using 3 %–5 % acetic acid. Well-preserved fossil specimens were selected using a stereomicroscope (BXT-1304E). For these specimens, scanning electron microscopy (SEM) imaging was performed at the Testing Center, College of Resources and Environmental Engineering, Guizhou University (COXEM-30: 20 kV and 3.48×10^{-5} Pa). All specimens are deposited at the Guizhou Provincial Key Laboratory for Palaeontology and Palaeoenvironment (Guizhou University), Guiyang, China. Specimen numbers and SEM stub numbers are available in Table S1 in the Supplement.

4 Results and discussion

4.1 Systematic palaeontology

The morphological terminology used here follows that of treatises on brachiopods (Williams et al., 2000). In our descriptions, we follow the suggestion in Pan et al. (2019) that the term "larval shell" as it is presented should be replaced by "metamorphic shell" (see Zhang et al., 2018a, b, for a full discussion). Ushatinskaya and Korovnikov (2016: p. 454) considered the "tubercles" of botsfordiid to be homologous in relation to the "setal lobes" of the metamorphic shell of other lingulid brachiopods. It is also considered to be the case that "pustule" is equivalent to "granule" and "pustulose" (Ushatinskaya and Korovnikov, 2016). Herein, we use pustule to indicate the dense and irregular ornaments on the surface of the post-metamorphic shell.

Subphylum Linguliformea Williams et al., 1996

Class Lingulata Gorjansky and Popov, 1985

Order Lingulida Waagen, 1885

Superfamily Acrotheloidea Walcott and Schuchert in Walcott, 1908

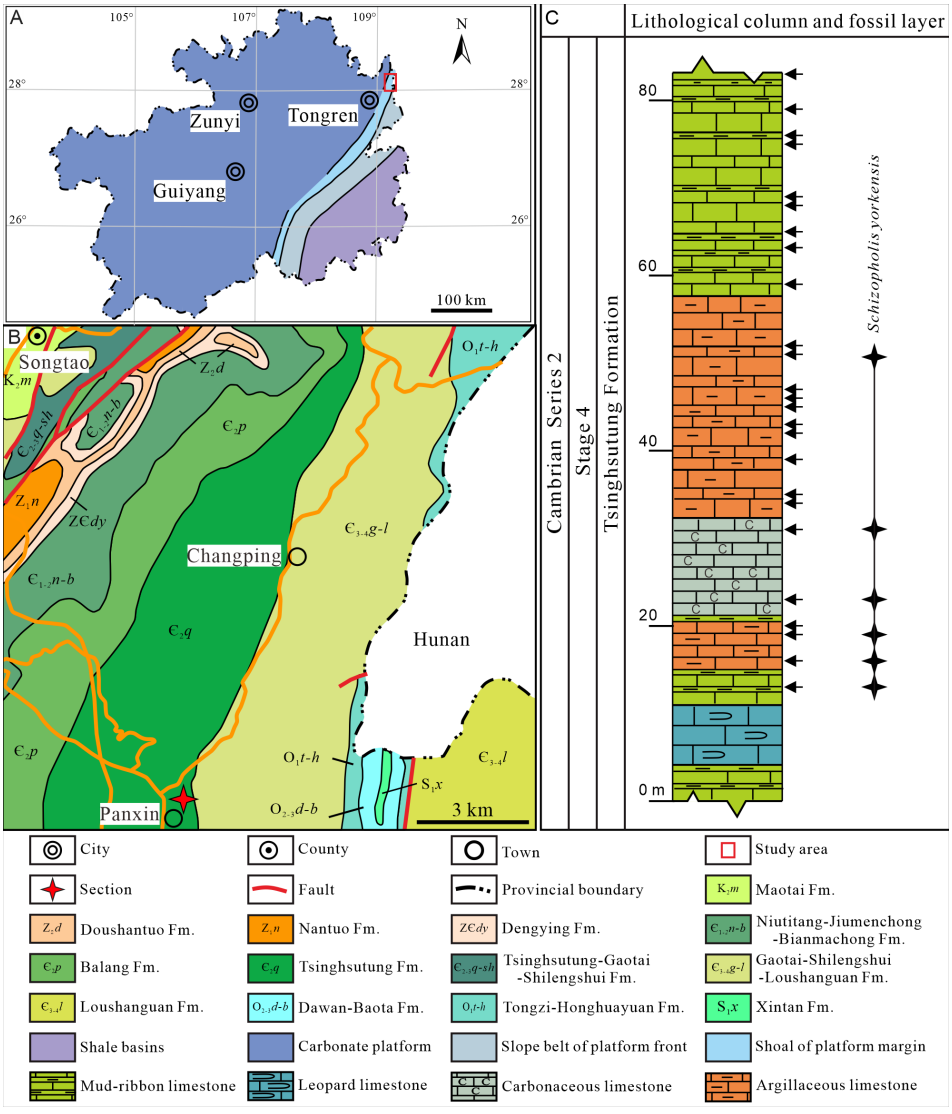

Figure 1. Lithofacies palaeogeographical, geological, and geographical maps showing the studied area, section, and lithological column and fossil layer. **(A)** Lithofacies palaeogeographical map of Guizhou Province (modified from Sang and Wang, 1987; Yin, 1990). **(B)** Geological and geographical maps of the study region (the four-pointed red star refers to the studied section). **(C)** Lithological column and fossil layer of *Schizopholis* from the Tsinghsutung Formation of Cambrian Series 2, Stage 4 at the Panxin section in Songtao County, Guizhou Province (the black arrows indicate sample layers, and the four-pointed black stars indicate fossil layers).

Family Botsfordiidae Schindewolf, 1955

Genus *Schizopholis* Waagen, 1885

Type species. *Schizopholis rugosa* Waagen, 1885, lower Cambrian, Khussak Formation (lower *Neobolus* beds), Salt Range, Pakistan.

Diagnosis. See Popov et al. (2015: p. 376) and Claybourn et al. (2020: p. 363).

Species included. In addition to the type species *S. rugosa* (Waagen, 1885), the genus *Schizopholis* contains the following species: *S. yorkensis* (Gravestock et al., 2001), *S. napuru* (Kruse, 1990), *S. quadrituberculum* (Percival and Kruse, 2014), *S. coronata* (Koneva, 1986), *S. kurtuju* (Kruse, 1998), *Schizopholis* sp. (Hu et al., 2021), and *Schizopholis*? sp. (Popov et al., 2021).

Schizopholis yorkensis Gravestock et al., 2001 (Figs. 2–5).

2001 *Karathele yorkensis* Gravestock et al., p. 128, pl. 21, figs. 1–11.

2006 *Karathele yorkensis* Jago et al., p. 415, figs. 4O–P.

2016 *Schizopholis yorkensis* Betts et al., p. 195, figs. 17A–H.

2019 *Schizopholis yorkensis* Betts et al., p. 502, fig. 11.

2019 *Schizopholis yorkensis* Pan et al., p. 524, fig. 9.

2020 *Schizopholis yorkensis* Claybourn et al., p. 364, figs. 9–10.

Material. Specimens collected include 2 hinged dorsal and ventral valves, 25 dorsal valves, and 23 ventral valves from the Tsinghsutung Formation of the Cambrian Series 2, Stage 4 at the Panxin section, Songtao County, Guizhou Province.

Diagnosis. See Ushatinskaya and Holmer in Gravestock et al. (2001, p. 128).

Description. Shell is small and circular or closely circular in outline, with maximum width near the mid-length (Figs. 2A–C, G, H; 4A, D; 5A, B, D). Both valves typically fragmented at anterior and lateral margins (Figs. 2–5). Metamorphic shell is close to circular in outline (Figs. 2A–C and 5A, D), covered by circular pits of varying diameters (Figs. 2F; 3E; 4C, F). Two types of pitting ornaments are observed on the metamorphic shell: small pits with diameters ranging from 0.5 to 3 µm, and large pits with diameters ranging from 3 to 7 µm (Figs. 2F, 3E, 4F). Two tubercles are on the dorsal metamorphic shell (Figs. 2A–E, 3A–D), whereas the ventral metamorphic shell shows a single high tubercle to the posterior (Fig. 4A–E) and two low tubercles to the anterior (dotted red line, Fig. 4A, B, D). The metamorphic shell is separated from the post-metamorphic shell by a halo, which is poorly developed on small specimens (Figs. 2A–E and 4A) but obviously developed on larger specimens (Figs. 3A–D and 4D). Post-metamorphic shell covered by numerous irregular pustules (∼ 7 µm in diameter on average; Figs. 2A–E; 3A–D; 4A, B, D, G), and well-developed growth lines seen in better-preserved, larger specimens (red arrows, Figs. 3A–C and 4B, D). Moreover, two shell layers are observed in the cross-section of the anterior edge of the post-metamorphic shell, namely the compact lamina of the primary layer and the columnar structures of the secondary layer (Fig. 3H), while pustules developed on the surface of the primary layer (Fig. 4G).

Dorsal valve is circular in outline (Fig. 2A–C, G, H), with approximate ratio of average width to length of 1.11 (width 287 to 1568 µm, Table 1). Dorsal metamorphic shell close to circular in outline (dotted white line, Figs. 2A–C and 3A–D), with approximate ratio of average width to length of 1.35 (length 236 to 408 µm and width 285 to 532 µm, Table 1). Dorsal metamorphic shell has two tubercles (Figs. 2A–E and 3A–D). The distance from the peak of each tubercle to the posterior margins is from 54 to 141 µm, and the distance between the two tubercles is from 82 to 161 µm (Table 1), and the two tubercles have nearly parallel arrangement (Figs. 2A–E and 3A–D). Dorsal post-metamorphic shell covered by numerous pustules (Figs. 2A–E and 3A–D). Median sulcus well-developed on the surface of post-metamorphic shell (Figs. 2A–C and 3A–C) and obvious on the larger specimens (Fig. 3A–C). Vestigial dorsal pseudointerarea, bisected by the shallow median groove (Figs. 2J and 3G). Dorsal interior develops a vestigial median septum extending to the mid-length of the valve (Figs. 2G, H and 3F) and obvious on the larger specimens (Fig. 3F). Central imprints of vestigial developed on both anterior sides of the median septum and obvious on the larger specimens (Fig. 3F), with paired transmedian imprints and *vascula lateralia* that are weakly developed in the interior of the dorsal valve but obviously well developed on the larger specimens (Fig. 3F).

Table 1. Average dimensions and ratios of dorsal valves of *Schizopholis yorkensis* from the Tsinghsutung Formation (Cambrian Series 2, Stage 4) at the Panxin section in Songtao County, Guizhou Province (unit: µm).

	L	W	L_m	W_m	L_{tu}	W_{tu}
N	14	15	16	17	14	17
Max	883	1568	408	526	141	161
Min	302	287	236	285	54	82
Mean	646	771	340	457	92	126
SD	165	280	49	55	29	21
	W/L	L_m/L	W_m/W	W_m/L_m	L_{tu}/L_m	W_{tu}/W_m
N	14	14	15	16	14	17
Max	1.71	0.87	0.99	1.68	0.35	0.31
Min	0.95	0.31	0.31	1.20	0.18	0.22
Mean	1.11	0.56	0.64	1.35	0.26	0.28
SD	0.19	0.15	0.16	0.14	0.06	0.03

Abbreviations: L – length of valve, W – width of valve, L_m – length of metamorphic shell, W_m – width of metamorphic shell, L_{tu} – length of the tubercle to the posterior margin, W_{tu} – width between two tubercles, N – number of specimens, Max – maximum value, Min – minimum value, Mean – average value, SD – standard deviation. Measurement data: Table S2.

Ventral valve is small, circular in outline, with maximum width near mid-length (Figs. 4A, D and 5A, B, D) and approximate ratio of average width to length of 1.14 (length 549 to 1856 µm and width 632 to 1918 µm, Table 2). Ventral metamorphic shell is rounded in outline (dotted white line, Fig. 4A, B, D), with an approximate ratio of average width to length of 1.28 (length 318 to 459 µm and width 397 to 580 µm, Table 2). Vestigial ventral pseudointerarea in small valves (Fig. 5A, B) and more obvious on larger valves (Fig. 5D). Vestigial ventral pseudointerarea in early stage and well developed later, divided by deep and wide pedicle groove (Figs. 4B, C and 5C, E). Pedicle groove forming a triangular delthyrium opening with divergent margins (Figs. 4A–E and 5C, E). Ventral visceral area usually vestigial and extends to one-third of the valve length (Fig. 5A, B, D).

Remarks. The morphological variability of *Schizopholis* is mainly in the number of tubercles on the metamorphic shell and the character of the pedicle opening (Kruse, 1990, 1998; Holmer et al., 1996, 2001; Gravestock et al., 2001; Percival and Kruse, 2014; Popov et al., 2015; Claybourn et al., 2020). *Schizopholis yorkensis* is similar to the type species *S. rugosa* and *S. napuru* in having two tubercles on the dorsal metamorphic shell and differs in having divergent delthyrium throughout the ontogeny of the ventral valve, while the latter two species have convergent delthyrium in the late pedicle opening but with a not completely merged margin (Table 3). *Schizopholis yorkensis* also has a wider triangular delthyrium

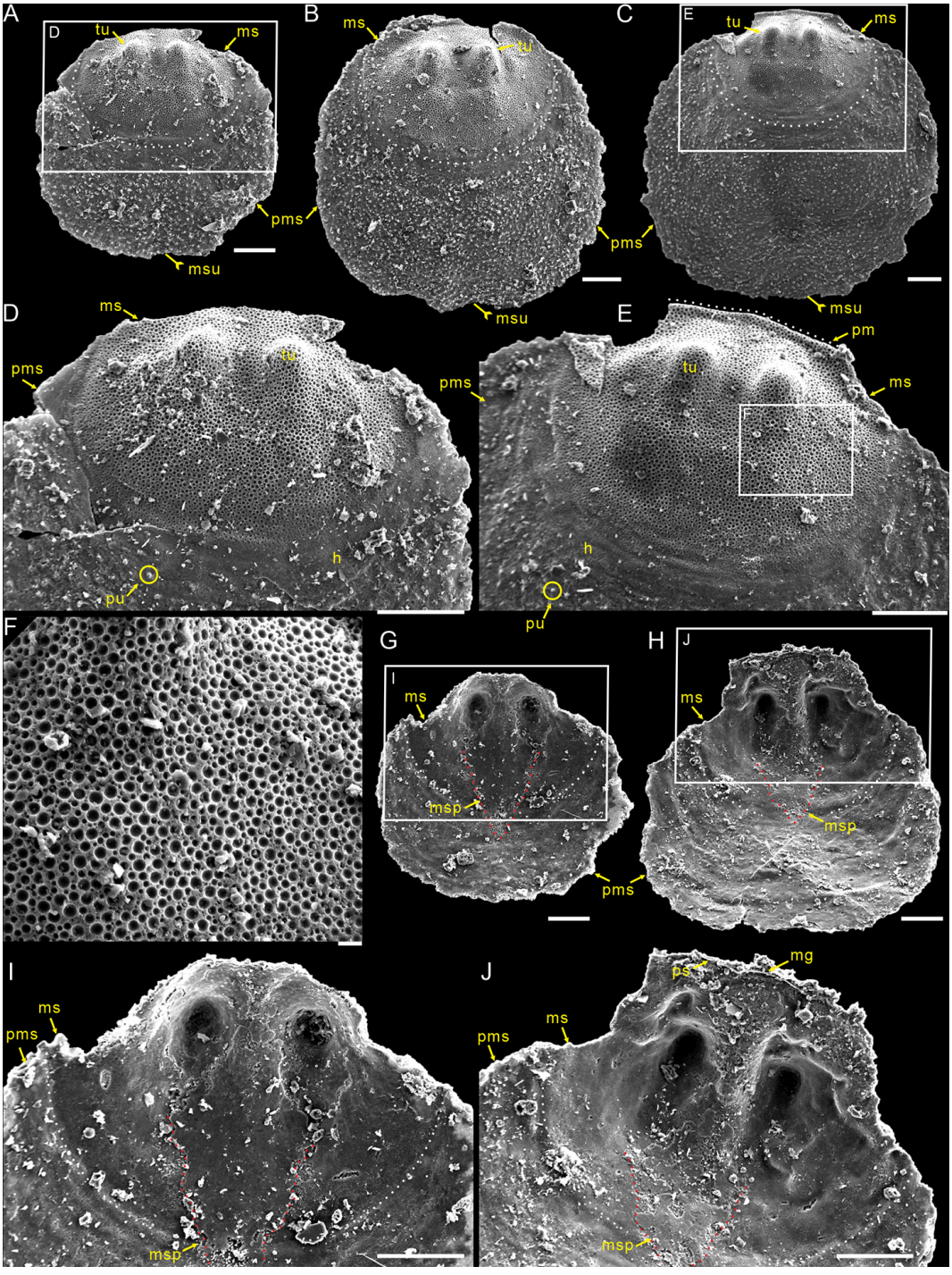

Figure 2. Small dorsal valves of *Schizopholis yorkensis* from the Tsinghsutung Formation (Cambrian Series 2, Stage 4) at the Panxin section in Songtao County, Guizhou Province, South China. **(A–C)** Exterior view, showing the subcircular circular in outline of the metamorphic shell, with two tubercles on the metamorphic shell and a median sulcus on the post-metamorphic shell: **(A)** PX–15m–401, **(B)** PX–15m–409, and **(C)** PX–15m–390. **(D)** Enlarged view of **(A)**, magnifying the metamorphic shell and showing the halo at the metamorphic shell boundary and pustules on the post-metamorphic shell. **(E)** Enlarged view of **(C)**, showing arcuately posterior margin (dotted white line). **(F)** Enlarged view of **(E)**, showing finely circular pits of varying diameters. **(G–H)** Interior view, showing the median septum extended to the mid-length of the shell: **(G)** PX–15m–421 and **(H)** PX–15m–408. **(I)** Enlarged view of **(G)**, with magnification of the median septum (dotted red line). **(J)** Enlarged view of **(H)**, showing vestigial pseudointerarea and shallowly median groove. The scale bars represent 100 µm **(A–E, G–J)** and 10 µm **(F)**. Abbreviations: gl – growth line, h – halo, mg – median groove, ms – metamorphic shell, msp – median septum, msu – median sulcus, pm – posterior margin, ps – pseudointerarea, pu – pustule, pms – post-metamorphic shell, tu – tubercle.

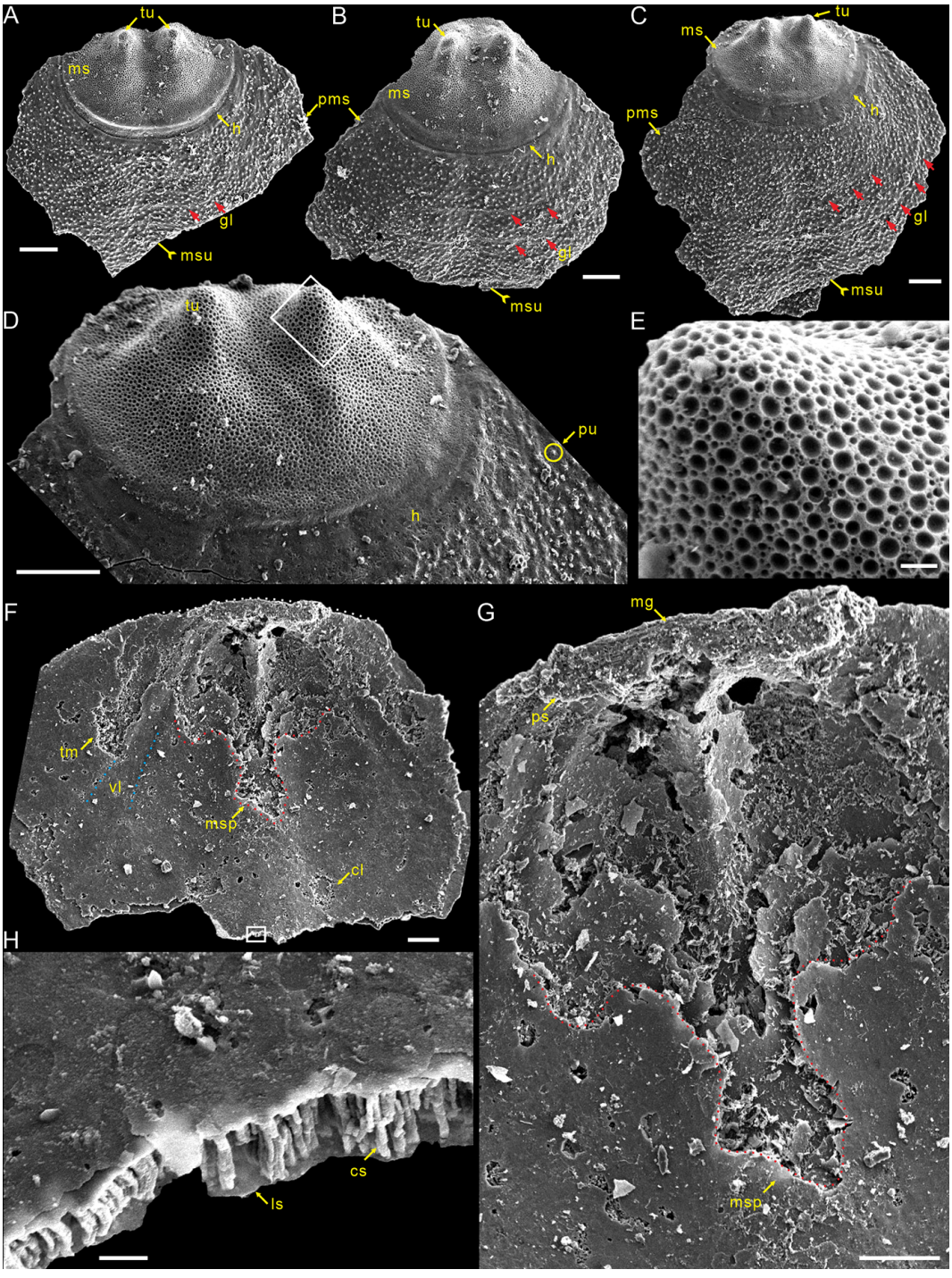

Figure 3. Large dorsal valves of *Schizopholis yorkensis* from the Tsinghsutung Formation (Cambrian Series 2, Stage 4) at the Panxin section in Songtao County, Guizhou Province, South China. **(A–C)** Exterior view, showing two tubercles on the metamorphic shell and growth lines (red arrow) on the post-metamorphic shell, as well as an obvious halo at the metamorphic shell boundary: **(A)** PX–15m–415, **(B)** PX–15m–395, and **(C)** PX–15m–391. **(D)** Enlarged view of **(C)**, showing two tubercles on the metamorphic shell, pustules on the post-metamorphic shell, and an obvious halo at the metamorphic shell boundary. **(E)** Enlarged view of **(D)**, showing finely circular pits of varying diameters. **(F)** PX–15m–271, interior view, showing arcuately posterior margin (dotted white line), paired transmedian imprints and central imprints, straight *vascula lateralia* (dotted blue line), and median septum (dotted red line). **(G)** Enlarged view of **(F)**, magnifying the median groove, pseudointerarea, and median septum. **(H)** Enlarged view of **(F)**, showing the lamina structure and columnar structure. The scale bars represent 100 µm **(A–D, F, G)** and 10 µm **(E, H)**. Abbreviations: cl – central imprints, cs – column structure, ls – lamina structure, mr – median ridge, tr – transmedian imprints, vl – *vascula lateralia*; for the other abbreviations, see Fig. 2.

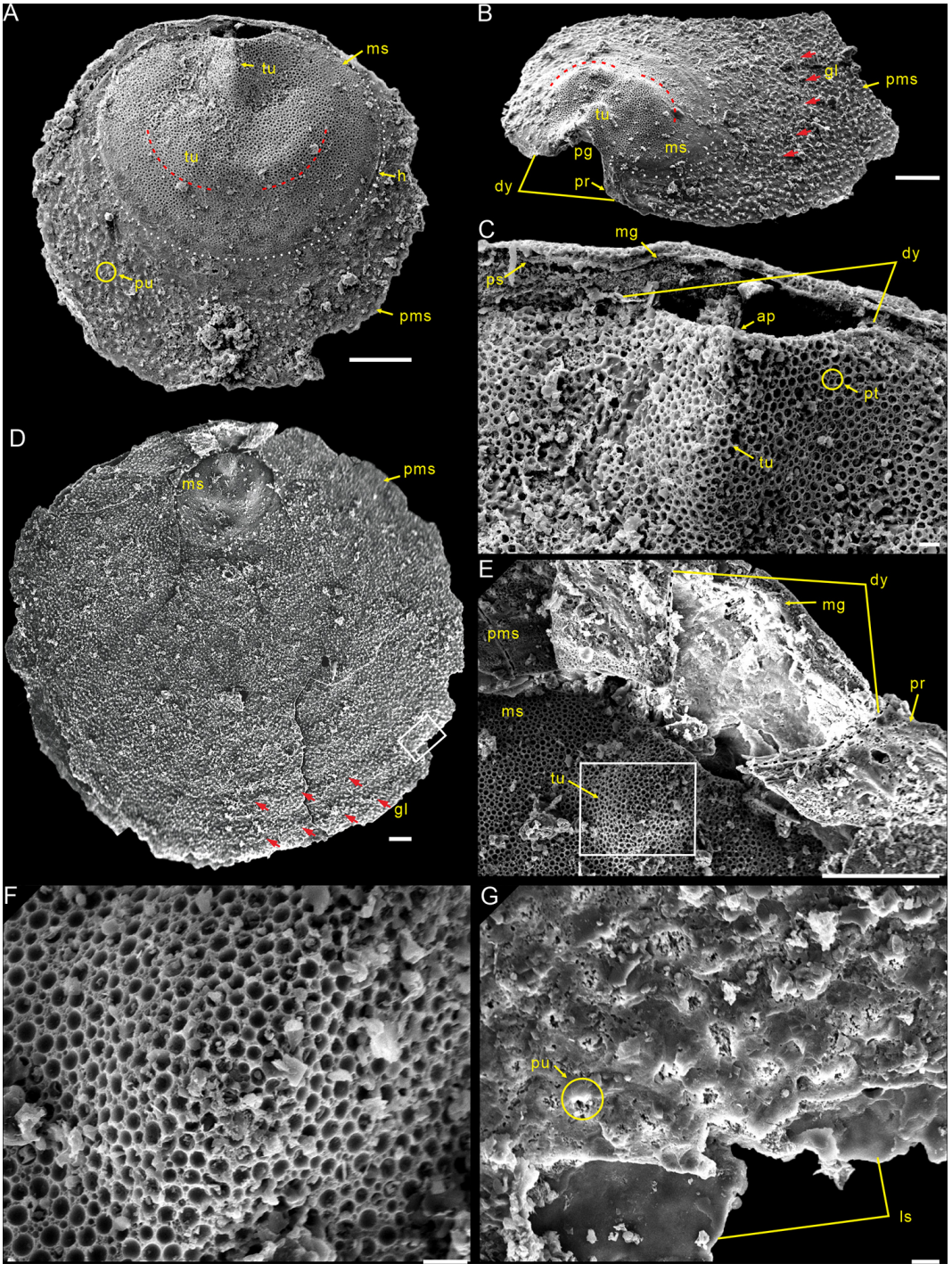

Figure 4. Ventral valves of *Schizopholis yorkensis* from the Tsinghsutung Formation (Cambrian Series 2, Stage 4) at the Panxin section in Songtao County, Guizhou Province, South China. **(A)** PX–14m–43, small specimen, showing the circular outline, with three tubercles on the metamorphic shell and pustules on the post-metamorphic shell. **(B)** PX–15m–274, lateral exterior view, showing open pedicle groove, divergent delthyrium, developed propareas, and growth lines (red arrow) on the post-metamorphic shell. **(C)** Enlarged view of **(A)**, showing the apex, the high tubercle and divergent delthyrium on the ventral valve, and the pseudointerarea and median groove on the dorsal valve. **(D)** PX–15m–351, large specimen, shown to be circular in terms of the outline of the metamorphic shell (dotted white line), with concentric growth lines (red arrow) on the post-metamorphic shell. **(E)** Enlarged view of **(D)**, showing the divergent delthyrium, developed propareas, and shallow median groove. **(F)** Enlarged view of **(E)**, showing circular pits of varying diameters. **(G)** Enlarged view of **(D)**, showing pustules on the post-metamorphic shell and lamina structure. The scale bars represent 100 µm **(A, B, D, E)** and 10 µm **(C, F, G)**. Abbreviations: ap – apex, dy – delthyrium, pg – pedicle groove, pr – proparea; for the other abbreviations, see Fig. 3.

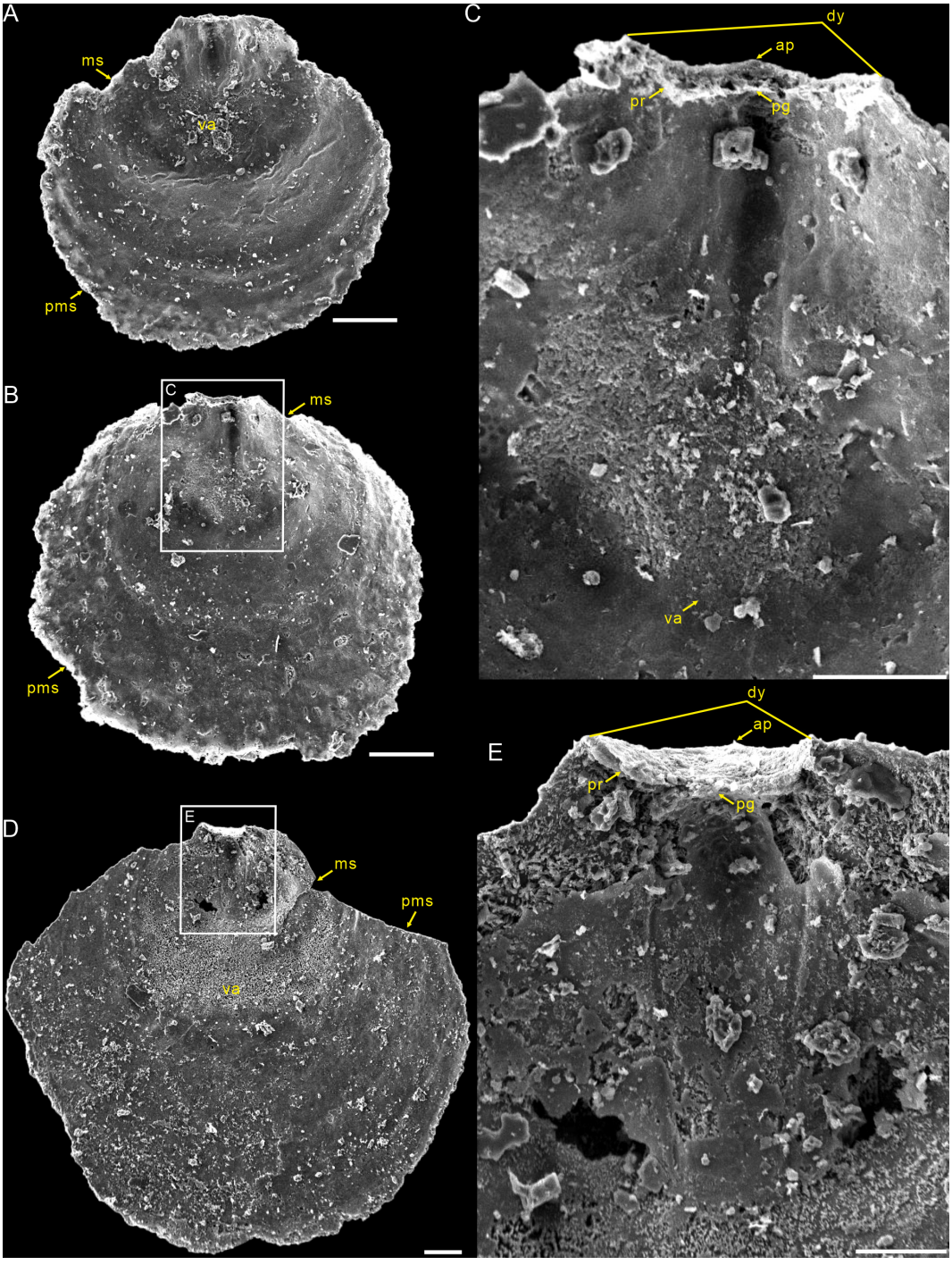

Figure 5. Interior views of the ventral valves of *Schizopholis yorkensis* from the Tsinghsutung Formation (Cambrian Series 2, Stage 4) at the Panxin section in Songtao County, Guizhou Province, South China. **(A–B)** Small specimens: **(A)** PX–15m-398 and **(B)** PX–15m–414. **(C)** Enlarged view of **(B)**, showing open pedicle groove, divergent delthyrium, apex, and vestigial proparea and visceral area. **(D)** PX–15m–393, large specimen. **(E)** Enlarged view of **(D)**, showing open pedicle groove, divergent delthyrium, apex, and developed proparea. The scale bars represent 100 µm **(A, C, D)** and 50 µm **(B, E)**. Abbreviation: va – visceral area; for the other abbreviations, see Fig. 4.

Table 2. Average dimensions and ratios of ventral valves of *Schizopholis yorkensis* from the Tsinghsutung Formation (Cambrian Series 2, Stage 4) at the Panxin section in Songtao County, Guizhou Province (unit: μm).

	L	W	L_m	W_m	W/L	L_m/L	W_m/W	W_m/L_m
N	15	15	15	15	15	15	15	15
Max	1856	1918	459	580	1.38	0.70	0.79	1.49
Min	549	632	318	397	0.90	0.20	0.23	1.13
Mean	910	1045	373	478	1.14	0.45	0.52	1.28
SD	334	405	34	52	0.15	0.14	0.18	0.13

Abbreviations: see Table 1. Measurement data: Table S3.

(Smith et al., 2015) and a smaller maximum size (Gravestock et al., 2001) as opposed to *S. napuru*. Additionally, *S. yorkensis* is similar to the species *S. coronata*, *S. quadrituberculum*, and *S. kurtuju* in having divergent delthyrium throughout its ontogeny, while the latter three species have four tubercles on their dorsal metamorphic shell (Table 3).

Schizopholis yorkensis was originally established and described by Ushatinskaya and Holmer (in Gravestock et al., 2001) based on specimens from the Parara Formation in Yorke Peninsula, South Australia. To date, *S. yorkensis* has been reported in Australia (Gravestock et al., 2001; Jago et al., 2006; Betts et al., 2016, 2019), North China (Pan et al., 2019), and Antarctica (Claybourn et al., 2020). In this paper, the species is firstly described in the limestones of the Tsinghsutung Formation in Songtao County, Guizhou Province, South China. The specimens are assigned to *Schizopholis yorkensis* because the shell is small (maximum length of 1856 μm, Table 2), with two tubercles on the dorsal metamorphic shell and three on the ventral metamorphic shell, as well as a well-developed broad and divergent delthyrium throughout the ontogeny of ventral valve (see Figs. 2–5). The specimens from the Tsinghsutung Formation are much smaller than *S. napuru* (maximum length of 7.6 mm, Kruse, 1990; Liu et al., 2020). The specimens are similar to *S. yorkensis* from Australia (Gravestock et al., 2001; Betts et al., 2016, 2019), Antarctica (Claybourn et al. 2020), and North China (Pan et al., 2019). However, the difference is that it is larger in terms of the size of the metamorphic shell than the Australia specimens (150–160 μm, Gravestock et al., 2001) but similar to those from North China (246–420 μm, Pan et al., 2019) and Australia (330–370 μm, Betts et al., 2019). These results show an overlap with the diameter of the metamorphic shell of the specimens from South China (236–459 μm, Tables 1–2).

4.2 Palaeogeographical distribution of *Schizopholis*

Schizopholis is currently known from Australia (Kruse, 1990, 1991, 1998; Brock and Cooper, 1993; Gravestock et al., 2001; Jago et al., 2006; Percival and Kruse, 2014; Smith et al., 2015; Betts et al., 2016, 2019), Antarctica (Holmer et al., 1996; Claybourn et al., 2020), the Himalaya (Popov et al., 2015), Kazakhstan (Koneva, 1986; Holmer et al., 2001; Popov et al., 2021), South China (Chen et al., 2019; Liu et al., 2020), and North China (Pan et al., 2019; Hu et al., 2021) (Fig. 6). Palaeogeographical analysis of *Schizopholis* indicates that the genus was distributed across East Gondwana, South China, North China, and Kazakhstan, with occurrences mainly being confined to low-latitude regions (Fig. 6A). Additionally, *Schizopholis* had a wide temporal distribution, ranging from Cambrian Age 3 to Guzhangian Age (Fig. 6). Based on the existing records, *Schizopholis* achieved the highest diversity level in Australia, where four species in total have been recognized: *S. napuru* (Kruse, 1990, 1991, 1998; Brock and Cooper, 1993; Smith et al., 2015), *S. yorkensis* (Gravestock et al., 2001; Jago et al., 2006; Betts et al., 2016, 2019), *S. quadrituberculum* (Percival and Kruse, 2014), and *S. kurtuju* (Kruse, 1998) (Fig. 6A). The species *S. yorkensis* and *S. napuru* are also found in Antarctica (Holmer et al., 1996; Claybourn et al., 2020) and South China (Liu et al., 2020; this paper) (Fig. 6A), which suggests close palaeobiogeographical relationships among South China, Australia, and Antarctica.

The earliest fossil record of *Schizopholis* is in the Cambrian Age 3, and there is only one species (*S. yorkensis*) with reports mainly from Australia (Jago et al., 2006; Betts et al., 2016) and North China (Pan et al., 2019) (Fig. 6A, B). However, during the Cambrian Age 4, the genus has a wider distribution and high diversity (Fig. 6A, B). Specifically, three species were found in Australia, namely *S. yorkensis*, *S. napuru*, and *S. quadrituberculum* (Kruse, 1990, 1991, 1998; Brock and Cooper, 1993; Gravestock et al., 2001; Jago et al., 2006; Percival and Kruse, 2014; Smith et al., 2015; Betts et al., 2019); two species were found in the Himalaya, namely *S. napuru* and *S. rugosa* (Popov et al., 2015); two species were found in Antarctica, namely *S. yorkensis* and *S. napuru* (Holmer et al., 1996; Claybourn et al., 2020); two species were found in South China, namely *S. yorkensis* and *S. napuru* (Liu et al., 2020; this paper), and one species was found in North China: *S. yorkensis* (Pan et al., 2019). In contrast, it shows less widespread distribution and lower diversity during the Wuliuan Age (Fig. 6A, B). Specifically, one species was found in Australia, namely *S. kurtuju* (Kruse, 1998); similarly, one species was found in Kazakhstan, namely *S.*

Table 3. Comparison of key morphological characteristics of *Schizopholis* species.

Species characteristic	*S. rugosa*	*S. napuru*	*S. yorkensis*	*S. quadritubercerculum*	*S. kurtuju*	*S. coronata*
Shell morphology	Closely similar to *S. napuru*	Circular (maximum know valve length 7.6 mm)	Circular or close to circular (length 0.7–1.0 mm)	Subcircular	Subcircular (maximum know valve length 10.4 mm)	Small, subcircular to slightly transversely suboval
Pits on MS	Preserve	Preserve	Preserve	Preserve	Preserve	Preserve
Tubercle number of dorsal MS	Two	Two	Two	Four	Four	Four
Tubercle number of ventral MS	/	Single of high posterior, two of high anterior	Single of high posterior, two of low anterior	Single posterior, two anterior	Single posterior, two anterior	Single posterior, two anterior
Pustules on PMS	Preserve	Preserve	Preserve	Preserve	Preserve	Preserve
Concentric growth lines on PMS	/	Preserve, more obvious when valve length beyond 4.0 mm	Preserve	Occasional confined to posterior	Preserve (valve length 7.0–7.5 mm)	Preserve
Median septum (ridge)	/	Median septum	Median ridge	Median tongue, well-developed divergent lateral ridges	Ridgelike, extends to about one-fifth valve length	Slender median ridge
Ventral apex	More marginal position than *S. napuru*	High, located at about one-sixth of the ventral valve length	Strongly elevated	High, located at about one-seventh of the valve length	Low, located at about 1/10 of the ventral valve length	/
Pedicle groove	/	Deep pedicle groove	Deep, forming a high delthyrium opening	Hemicylindrical pedicle groove	Shallower pedicle groove	Deep, short; shallower than *S. napuru*
Late pedicle opening	Convergent delthyrium but not completely merged	Convergent delthyrium but not completely merged	Divergent delthyrium throughout ontogeny	Divergent delthyrium throughout ontogeny	Open, persistently widening	Divergent delthyrium
Reference	Popov et al. (2015)	Kruse (1990, 1998)	Gravestock et al. (2001)	Percival and Kruse (2014)	Kruse (1998)	Holmer et al. (2001)

Abbreviations: S. – *Schizopholis*, MS – metamorphic shell, PMS – post-metamorphic shell.

coronata (Holmer et al., 2001). During the Drumian Age, the species diversity was even lower, with only one species being found in Kazakhstan: *S. coronata* (Holmer et al., 2001) (Fig. 6A, B). Additionally, an unnamed species of *Schizopholis* has been recorded in Kazakhstan, with its geological age ranging from the Cambrian Age 4 to the Wuliuan Age (Popov et al., 2021) (Fig. 6A, B). In North China, there is also an unnamed species of *Schizopholis* that has been found from the Drumian to the Guzhangian Age (Hu et al., 2021). Based on the analysis of the distribution of *Schizopholis*, we found that only one species occurred in the Cambrian Age 3, four species occurred in the Cambrian Age 4, two species occurred in the Wuliuan Age, and only one species occurred in the Drumian Age. The results show that *Schizopholis* had a high diversity during the Cambrian Age 4 (Fig. 6A, B), suggesting that the diversity of the genus had a rapid expansion trend during this period and then gradually decreased in the Wuliuan to the Guzhangian Age.

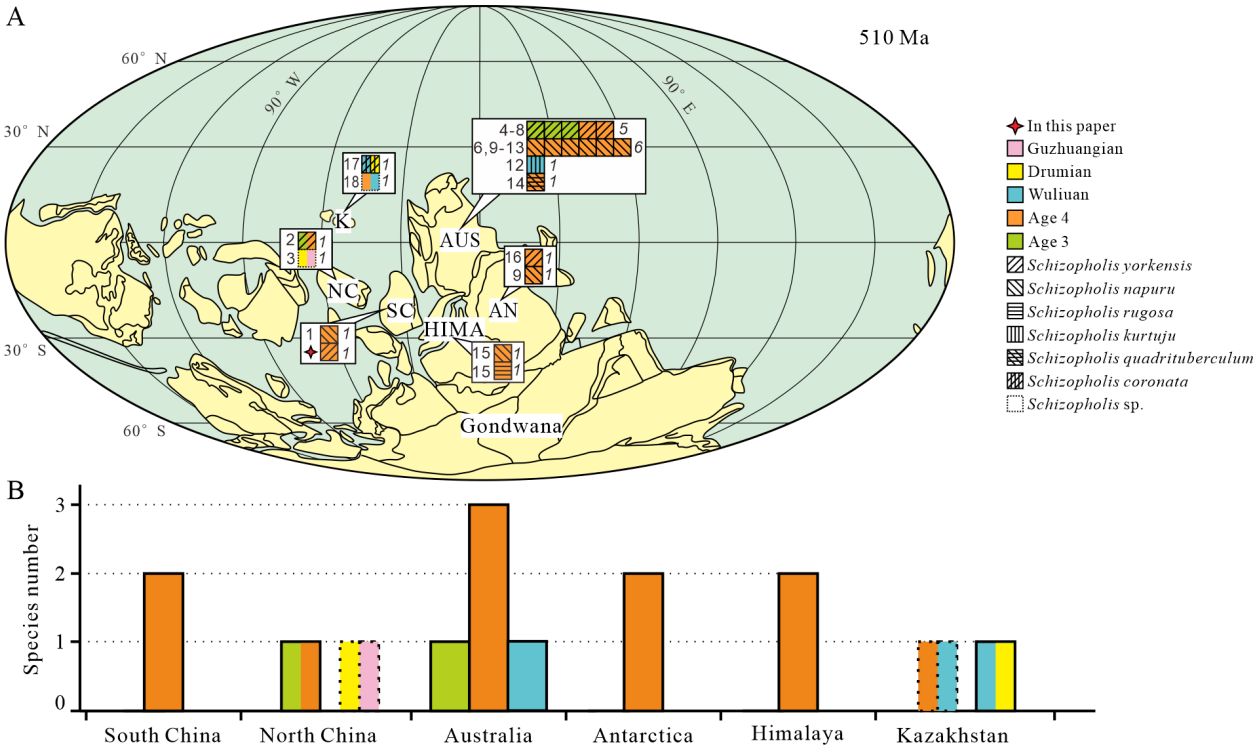

Figure 6. Palaeogeographical distribution and diversity of *Schizopholis* in the Cambrian. **(A)** Palaeogeographical distribution of *Schizopholis* species during the Cambrian Age 3 to the Guzhangian Age: italic numbers represent the abundance of *Schizopholis*, and roman numbers indicate the literature numbers (palaeogeographic reconstruction is modified from Torsvik and Cocks, 2017; Yang et al., 2015). **(B)** Diversity of *Schizopholis* during the Cambrian Age 3 to the Guzhangian Age. Abbreviations: NC – North China, SC – South China, K – Kazakhstan, AUS – Australia, AN – Antarctica, HIMA – Himalaya. Literature numbers: (1) Liu et al. (2020), (2) Pan et al. (2019), (3) Hu et al. (2021), (4) Betts et al. (2019), (5) Jago et al. (2006), (6) Brock and Cooper (1993), (7) Betts et al. (2016), (8) Gravestock et al. (2001), (9) Holmer et al. (1996), (10) Smith et al. (2015), (11) Kruse (1990), (12) Kruse (1998), (13) Kruse (1991), (14) Percival and Kruse (2014), (15) Popov et al. (2015), (16) Claybourn et al. (2020), (17) Holmer et al. (2001), (18) Popov et al. (2021).

4.3 Biostratigraphical correlation implications of *Schizopholis*

Trilobites play an important role in biostratigraphical correlations in the Cambrian, and well-established trilobite zones in regions such as South China, North China, Australia, and the Himalaya effectively facilitate biostratigraphic correlation (Peng et al., 2009; Popov et al., 2015; Zhu et al., 2019; Zhao et al., 2019; Geyer, 2020) (Fig. 7). However, no trilobite zone has been established in Antarctica (Holmer et al., 1996). Notably, a brachiopod assemblage, including *Eoobolus* aff. *elatus*, *Schizopholis napuru*, and *Vandalotreta djagoran*, found in glacial erratics from the Miocene glaciomarine Cape Melville Formation of King George Island, Antarctica, is closely similar to that from the Wirrealpa and Aroona Creek Limestones in Australia (Brock and Cooper, 1993; Holmer et al., 1996). Significantly, *Schizopholis* and *Eoobolus* were also recorded in the Shackleton Limestone of the Byrd Group in the Central Transantarctic Mountains of Antarctica (Claybourn et al., 2020). Furthermore, Claybourn et al. (2021) suggested that the small shelly fossil (SSF) assemblage containing brachiopod from the upper Shackleton Limestone of the Byrd Group in Antarctica was correlated with the *Dailyatia odyssei* Zone (SSF) and the trilobite *Pararaia janeae* Zone of Australia. Concurrently, the biostratigraphic significance of brachiopods has attracted considerable attention (Popov et al., 2015; Hughes, 2016; Betts et al., 2017; Pan et al., 2019; Holmes et al., 2025).

Both *Schizopholis yorkensis* and *S. napuru* are the most widely distributed species in this genus. The earliest *S. yorkensis* was reported from the trilobite *Pararaia tatei* zone of Australia (Jago et al., 2006; Betts et al., 2016, 2017) and the Xinji Formation of North China (Pan et al., 2019) in the Cambrian Age 3 (Fig. 7). On the other hand, during the Cambrian Age 4, *S. yorkensis* expanded beyond Australia (Brock and Cooper, 1993; Gravestock et al., 2001; Betts et al., 2019) and North China (Pan et al., 2019) to regions such as South China (this study) and Antarctica (Claybourn et al., 2020) (Figs. 6–7). Additionally, *S. napuru* was also widespread, identified in Australia (Brock and Cooper, 1993; Kruse, 1990, 1991, 1998; Smith et al., 2015), Antarctica (Holmer et al., 1996), the Lesser Himalaya (Popov et al., 2015), and South China (Liu et al., 2020), during the Cam-

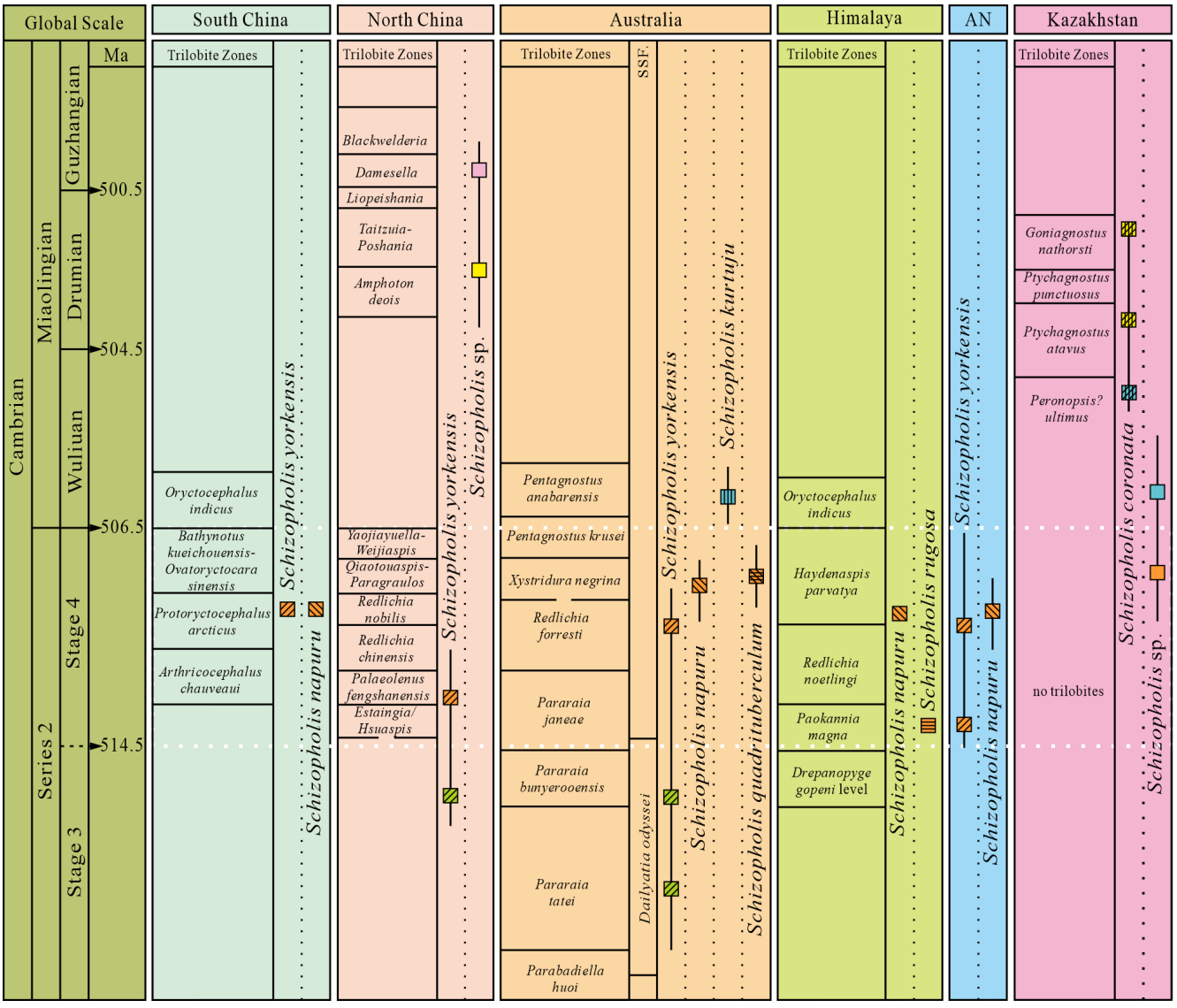

Figure 7. The distribution and occurrence horizon of *Schizopholis* from the Cambrian Stage 3 to Guzhangian (Trilobite zone date from Peng et al., 2009; Popov et al., 2015; Zhu et al., 2019; Zhao et al., 2019; Geyer, 2020). Abbreviations: AN – Antarctica, SSF – small shelly fossil.

brian Age 4 (Figs. 6–7). In comparison with *S. yorkensis*, *S. napuru* has a shorter stratigraphic range, making it more useful than *S. yorkensis* for global biostratigraphical correlation.

In Australia, *Schizopholis napuru* is widespread in various locations, including the Tindall Limestone in the Daly Basin (Kruse, 1990), the Top Springs Limestone and Gum Ridge Formation in the Georgina Basin (Kruse, 1991, 1998), the Wirrealpa Limestone in the Arrowie Basin (Brock and Cooper, 1993), the Montejinni Limestone in the Wiso Basin (Kruse, 1998), and the Tempe Formation in the Amadeus Basin (Smith et al., 2015). Holmes et al. (2025) defined a new organophosphatic brachiopod *Schizopholis napuru* zone in Australia, which is equivalent to the trilobite *Xystridura negrina* zone. On the other hand, *S. napuru* has also been identified in the Parahio Formation of the Parahio Valley in the Himalaya within the lower *Haydenaspis parvaya* zone (Popov et al., 2015) (Fig. 7). Additionally, Liu et al. (2020) described *S. napuru* to be occurring in the trilobite *Protoryctocephalus arcticus* zone of the Tsinghsutung Formation in South China (Fig. 7). Moreover, *S. napuru* is also reported in glacial erratic boulders within the Cape Melville Formation on King George Island, Antarctica (Holmer et al., 1996) (Fig. 7). Thus, the distribution of *Schizopholis* suggests that *S. napuru* may prove to be an important indicator for biostratigraphical correlations within the Cambrian Stage 4 (Fig. 7), especially in those areas where trilobites are absent.

5 Conclusions

In this study, we systematically described, for the first time, *Schizopholis yorkensis* from the Tsinghsutung Formation (Cambrian Series 2, Stage 4) in Songtao County, Guizhou Province, South China.

Analysis of the palaeobiogeographical distribution of *Schizopholis* shows that this genus is predominantly distributed at low-latitude regions and reached its highest abundance/diversity level during the Cambrian Age 4. Notably, results showed the co-occurrence of *S. yorkensis* and *S. napuru* in Australia, Antarctica, and South China, suggesting closely palaeobiogeographic relationships among these three continents.

In addition, both *Schizopholis napuru* and *S. yorkensis* are globally distributed. However, *S. napuru* has a shorter geological time range, occurring primarily within the Cambrian Age 4. Thus, it may provide important support for biostratigraphical correlation within this time interval.

Data availability. The material can be accessed at the Guizhou Provincial Key Laboratory for Palaeontology and Palaeoenvironment (Guizhou University), Guiyang, China. Data are shown in Tables S1–S3.

Supplement. The supplement related to this article is available online at https://doi.org/10.5194/jm-45-259-2026-supplement.

Author contributions. BQW: investigation and writing (original draft preparation). BQW and DZW: formal analysis, methodology, and software. BQW and XLY: data curation and visualization conceptualization. XLY, WYW, and YQM: validation, resources, data curation, project administration, supervision, funding acquisition, and writing (review and editing). All of the authors contributed to and approved the initially submitted version of the paper.

Competing interests. The contact author has declared that none of the authors has any competing interests.

Disclaimer. Publisher's note: Copernicus Publications remains neutral with regard to jurisdictional claims made in the text, published maps, institutional affiliations, or any other geographical representation in this paper. The authors bear the ultimate responsibility for providing appropriate place names. Views expressed in the text are those of the authors and do not necessarily reflect the views of the publisher.

Acknowledgements. We sincerely thank Wenjie Jiang of the laboratory of Guizhou University for his technical guidance on the scanning electron microscopy. Thanks are given to Kerry Brown for the English language revisions of the paper. Many thanks are also extended to Rong Feng, Kailun Wu, and Zhenhua Zhou for their generous help with the field samples and fossil collection. We would also like to thank the editor and reviewers for useful comments that enhanced the paper.

Financial support. This work was supported by research grants from the National Natural Sciences Foundation of China (grant nos. 42262003, 42330209, and 42262002) and the Guizhou Science and Technology Fund (grant nos. Gui. Sci. Bas. ZD[2025]100 and Gui. Sci. Plat. ZSYS [2024]002).

Review statement. This paper was edited by Luke Mander and reviewed by Zhiliang Zhang and Yue Liang.

References

Bassett, M. G., Popov, L. E., and Holmer, L. E.: Organophosphatic brachiopods: Patterns of biodiversification and extinction in the early Palaeozoic, Geobios, 32, 145–163, https://doi.org/10.1016/S0016-6995(99)80026-6, 1999.

Betts, M. J., Paterson, J. R., Jago, J. B., Jacquet, S. M., Skovsted, C. B., Topper, T. P., and Brock, G. A.: A new lower Cambrian shelly fossil biostratigraphy for South Australia, Gondwana Research, 36, 176–208, https://doi.org/10.1016/j.gr.2016.05.005, 2016.

Betts, M. J., Paterson, J. R., Jago, J. B., Jacquet, S. M., Skovsted, C. B., Topper, T. P., and Brock, G. A.: Global correlation of the early Cambrian of South Australia: Shelly fauna of the *Dailyatia odyssei* Zone, Gondwana Research, 46, 240–279, https://doi.org/10.1016/j.gr.2017.02.007, 2017.

Betts, M. J., Claybourn, T. M., Brock, G. A., Jago, J. B., Skovsted, C. B., and Paterson, J. R.: Shelly fossils from the lower Cambrian White Point Conglomerate, Kangaroo Island, South Australia, Acta Palaeontologica Polonica, 64, 489–522, https://doi.org/10.4202/app.00586.2018, 2019.

Brock, G. A. and Cooper, B. J.: Shelly Fossils from the Early Cambrian (Toyonian) Wirrealpa, Aroona Creek, and Ramsay Limestones of South Australia, Journal of Paleontology, 67, 758–787, https://doi.org/10.1017/S0022336000037045, 1993.

Carlson, S. J.: The Evolution of Brachiopoda, Annual Review of Earth and Planetary Sciences, 44, 409–438, https://doi.org/10.1146/annurev-earth-060115-012348, 2016.

Chen, F. Y., Zhang, Z. F., Betts, M. J., Zhang, Z. L., and Liu, F.: First report on Guanshan Biota (Cambrian Stage 4) at the stratotype area of Wulongqing Formation in Malong County, Eastern Yunnan, China, Geoscience Frontiers, 10, 1459–1476, https://doi.org/10.1016/j.gsf.2018.09.010, 2019.

Claybourn, T. M., Skovsted, C. B., Holmer, L. E. Pan, B., Myrow, P. M., Topper, T., and Brock, G. A.: Brachiopods from the Byrd Group (Cambrian Series 2, Stage 4) Central Transantarctic Mountains, East Antarctica: Biostratigraphy, Phylogeny and Systematics, Papers in Palaeontology, 6, 349–383, https://doi.org/10.1002/spp2.1295, 2020.

Claybourn, T. M., Skovsted, C. B., Betts, M. J., Holmer, L. E., Bassett-Butt, L., and Brock, G. A.: Camenellan tommotiids from the Cambrian Series 2 of East Antarctica: Biostratigraphy, palaeobiogeography, and systematic, Acta Palaeontologica

Polonica, 66, 207–229, https://doi.org/10.4202/app.00758.2020, 2021.

Geyer, G.: A comprehensive Cambrian correlation chart, International Union of Geological Sciences, 42, 321–332, https://doi.org/10.18814/epiiugs/2019/019026, 2020.

Gravestock, D. I., Alexander, E. M., Demidenko, Y. E., Esakova, N. B., Holmer, L. E., Jago, J. B., Lin, T. R., Melnikova, N., Parkhaev, P. Y., Rozanov, A. Y., Ushatinskaya, G. T., Zang, W. L., Zhegallo, E. A., and Zhuravlev, A. Y.: The Cambrian biostratigraphy of the Stansbury Basin, South Australia, Transactions of the Palaeontological Institute of the Russian Academy of Sciences, 282, 1–345, ISBN 5784600958, 2001.

Gorjansky, V. Y. and Popov, L. E.: The morphology, systematic position and origin of inarticulate brachiopods with calcareous shells, Paleontological Journal, 3, 1–11, 1985.

Harper, D. A. T., Popov, L. E., and Holmer, L. E.: Brachiopods: Origin and early history, Palaeontology, 60, 609–631, https://doi.org/10.1111/pala.12307, 2017.

Holmer, L. E., Popov, L. E., and Wrona, R.: Early Cambrian lingulate brachiopods from glacial erratics of King George Island (South Shetland Islands), Antarctica, Palaeontologia Polonica, 55, 37–50, 1996.

Holmer, L. E., Popov, L. E., Koneva, S. P., and Bassett, M. G.: Cambrian–Early Ordovician Brachiopods from Malyi Karatau, the Western Balkhash region, and Tien Shan, Central Asia, Special Papers in Palaeontology, 65, 1–180, https://repository.geologyscience.ru/handle/123456789/26404 (last access: 7 April 2026), 2001.

Holmes, J. D., Smith, P. M., Paterson, J. R., Brock, G. A., and Betts, M. J.: The Cambrian Series 2–Miaolingian boundary interval in Australia: Biostratigraphic subdivision and implications for global multi-proxy correlation, Earth–Science Reviews, 265, 1–27, https://doi.org/10.1016/j.earscirev.2025.105106, 2025.

Hu, Y. Z., Holmer, L. E., Liang, Y., Duan, X. L., and Zhang, Z. F.: First Report of Small Shelly Fossils from the Cambrian Miaolingian Limestones (Zhangxia and Hsuzhuang Formations) in Yiyang County, Henan Province of North China, Minerals, 11, 1104, https://doi.org/10.3390/min11101104, 2021.

Hughes, N. C.: The Cambrian palaeontological record of the Indian subcontinent, Earth–Science Reviews, 159, 428–461, https://doi.org/10.1016/j.earscirev.2016.06.004, 2016.

Jago, J. B., Zang, W. L., Sun, X. W., Brock, G. A., Paterson, J. R., and Skovsted, C. B.: A review of the Cambrian biostratigraphy of South Australia, Palaeoworld, 15, 406–423, https://doi.org/10.1016/j.palwor.2006.10.014, 2006.

Koneva, S. P.: Some Middle and Late Cambrian inarticulate brachiopods in the Maly Karatau (southern Kazakhstan). Trudy Instituta Geologii i Geofiziki, Akademiya Nauk SSSP, Sibirskoye Otdelenye, 669, 201–209, 1986.

Korovnikov, I. V.: Early and middle Cambrian phylogeny of Acrothelidae brachiopods, Russian Geology and Geophysics, 39, 94–99, 1998.

Kruse, P. D.: Cambrian Palaeontology of the Daly Basin, Northern Territory Geological Survey Report, 7, 1–58, ISBN 0724514759, 1990.

Kruse, P. D.: Cambrian fauna of the Top Springs Limestone, Georgina Basin. The Beagle: Records of the Museums and Art Galleries of the Northern Territory, 8, 169–188, https://doi.org/10.5962/p.262819, 1991.

Kruse, P. D.: Cambrian palaeontology of the eastern Wiso and western Georgina Basins, Northern Territory Geological Survey Report, 9, 1–68, ISBN 0724534075, 1998.

Lin, H. L., Wang, J. G., and Liu, Y. R.: Cambrian strata in Songtao of Tongren, Guizhou and Luxi, Hunan Province, Journal of Stratigraphy, 1, 4–23, https://doi.org/10.19839/j.cnki.dcxzz.1966.01.003, 1966.

Liu, Y. J., Peng, J., Zhao, Y. L., and Mao, Y. Q.: First report of *Schizopholis* (Lingulata, Brachiopoda) from the Tsinghsutung Formation (Cambrian Series 2, Stage 4) in Guizhou, China, Palaeoworld, 30, 422–429, https://doi.org/10.1016/j.palwor.2020.07.006, 2020.

Pan, B., Skovsted, C. B., Brock, G. A., Topper, T. P., and Li, G. X.: Early Cambrian organophosphatic brachiopods from the Xinji Formation, at Shuiyu Section, Shanxi Province, North China, Palaeoworld, 29, 512–533, https://doi.org/10.1016/j.palwor.2019.07.001, 2019.

Peng, S. C., Hughes N. C., Heim, N. A., Sell, B. K., Zhu, X. J., Myrow, P. M., and Parcha, S. K.: Cambrian Trilobites from the Parahio and Zanskar Valleys, Indian Himalaya, Journal of Paleontology, 83, 1–95, https://doi.org/10.1666/08-129.1, 2009.

Percival, I. G. and Kruse, P. D.: Middle Cambrian brachiopods from the southern Georgina Basin of central Australia, Memoirs of the Association of Australasian Palaeontologists, 45, 349–402, https://search.informit.org/doi/10.3316/informit.345055178365213 (last access: 7 April 2026), 2014.

Popov, L. E., Holmer, L. E., Hughes, N. C., Ghobadi P. M., and Myrow, P. M.: Himalayan Cambrian brachiopods, Papers in Palaeontology, 1, 345–399, https://doi.org/10.1002/spp2.1017, 2015.

Popov, L. E., Nikitina, O. I., Pirogova, T. E., and Ergaliev, G. K.: Cambrian brachiopods from the area of the former Semipalatinsk nuclear–testing site, Chingiz Ranges, Kazakhstan, Palaontologische Zeitschrift, 95, 275–290, https://doi.org/10.1007/s12542-020-00540-9, 2021.

Sang, T. and Wang, L. T.: General Paleogeographic Situations, in: Regional Geology of Guizhou Province, Burean of Guizhou Geology, Mineral Resources, Geological Publishing House, Beijing, China, 480–483, https://xueshu.baidu.com/u/citation?type=txt&paperid=a762f72399dfa89d481c9b74dfcc2199 (last access: 7 April 2026), 1987.

Schindewolf, O. H.: Über einige kambrische Gattungen inartikulater Brachiopoden, Neues Jahrbuch für Mineralogie, Geologie and Paläontologie, 12, 538–557, 1955.

Smith, P. M., Brock, G. A., and Paterson, J. R.: Fauna and Biostratigraphy of the Cambrian (Series 2, Stage 4; Ordian) Tempe Formation (Pertaoorrta Group), Amadeus Basin, Northern Territory. Alcheringa An Australasian, Journal of Palaeontology, 39, 40–70, https://doi.org/10.1080/03115518.2014.951917, 2015.

Torsvik, T. H. and Cocks, L. R. M.: Earth History and Palaeogeography, Cambridge University Press, Cambridge, 317 pp., ISBN 9781107105324, 2017.

Ushatinskaya, G. T. and Korovnikov, I. V.: Revision of the superfamily Acrotheloidea (Brachiopoda, Class Linguliformea, Order Lingulida) from the Lower and Middle Cambrian of the Siberian Platform, Paleontological Journal, 50, 450–462, https://doi.org/10.1134/S0031030116050130, 2016.

Waagen, W. H.: Part 4: Brachiopoda, in: Salt Range fossils: Productus Limestone fossils, Memoirs of the Geological Survey of India (Palaeontologia Indica), 1, 329–770, 1885.

Walcott, C. D.: Cambrian Brachiopoda, descriptions of new genera and species, in: Cambrian geology and paleontology, Smithsonian Miscellaneous Collections, 53, 53–137, 1908.

Wei, B. Q., Yang, X. L., Cao, P., and Feng, R.: The discovery of *Eohadrotreta zhenbaensis* (Brachiopoda) from the Cambrian Series 2 Tsinghsutung Formation of Songtao, Guizhou, Acta Palaeontologica Sinica, 59, 163–170, https://doi.org/10.19800/j.cnki.aps.2020.02.03, 2020.

Wei, B. Q., Wang, Y., Yang, X. L., and Wu, W. Y.: The First Report of the Acrotretoid Brachiopod *Hadrotreta* from the Tsinghsutung Formation Cambrian (Series 2, Stage 4), Guizhou, South China, Biology–Basel, 12, 1083, https://doi.org/10.3390/biology12081083, 2023.

Williams, A., Carlson, S. J., Brunton, C. H. C., Holmer, L. E., and Popov, L. E.: A supra–ordinal classification of the Brachiopoda, Philos. Trans. R. Soc. B Biol. Sci., 351, 1171–1193, https://doi.org/10.1098/rstb.1996.0101, 1996.

Williams, A., Carlson, S. J., and Brunton, C. H. C.: Part H. Brachiopoda, in: Treatise on Invertebrate Paleontology, edited by: Kaesler, R. L., The Geological Society of America, Institute and The University of Kansas, Boulder, Colorado, and Lawrence, Kansas, 1–97, ISBN 0-8137-3108-9, 2000.

Yang, B., Steiner, M., and Keupp, H.: Early Cambrian palaeobiogeography of the Zhenba–Fangxian Block (South China): independent terrane or part of the Yangtze Platform?, Gondwana Res., 28, 1543–1565, https://doi.org/10.1016/j.gr.2014.09.020, 2015

Yin, G. Z.: Cambrian, in: Regional Geology of Guizhou province, edited by: Bureau of Guizhou Geology and Mineral Resources, Geological Publishing House, Beijing, China, 49–96, https://xueshu.baidu.com/u/citation?type=txt&paperid=a762f72399dfa89d481c9b74dfcc2199 (last access: 7 April 2026), 1987.

Yin, G. Z.: The Cambrian Divisions of Guizhou, Geology of Guizhou, 7, 283–292, 1990.

Zhang, Z. L., Zhang, Z. F., Holmer, L. E., and Chen, F. Y.: Post–metamorphic allometry in the earliest Acrotretoid brachiopods from the lower Cambrian (Series 2) of South China, and its implications, Palaeontology, 61, 183–207, https://doi.org/10.1111/pala.12333, 2018a.

Zhang, Z. L., Popov, L. E., Holmer, L. E., and Zhang, Z. F.: Earliest ontogeny of early Cambrian Acrotretoid brachiopods–First evidence for metamorphosis and its implications, BioMed Central Evolutionary Biology, 18, https://doi.org/10.1186/s12862-018-1165-6, 2018b.

Zhao, Y. L., Peng, S. C., Yuan, J. L., Esteve, J., Yang, X. L., Wu, M. Y., and Chen, Z. P.: The trilobite biostratigraphy for the Balang and "Tsinghsutung" formations, Cambrian Series 2, Stage 4 in the Balang area, Jianhe, Guizhou, South China, Estudios Geológicos, 75, e119, https://doi.org/10.3989/egeol.43595.574, 2019.

Zhu, M. Y., Yang, A. H., Yuan, J. L., Li, G. X., Zhang, J. M., Zhao, F. C., Ahn, S. Y., and Miao, L. Y.: Cambrian integrative stratigraphy and timescale of China, Science China Earth Sciences, 62, 25–60, https://doi.org/10.1007/s11430-017-9291-0, 2019.